Journal of Environmental Chemical Engineering 9 (2021) 105947

Contents lists available at ScienceDirect

Journal of Environmental Chemical Engineering

journal homepage: www.elsevier.com/locate/jece

Enhancement of nitrite/ammonia removal from saline recirculating aquaculture wastewater system using moving bed bioreactor

Musa Abubakar Tadda [a,b], Changwei Li [a], Mostafa Gouda [a,c], Abd El-Fatah Abomohra [d], Abubakar Shitu [a,b], Amimul Ahsan [e], Songming Zhu [a], Dezhao Liu [a,*]

[a] Key Laboratory of Equipment and Informatization in Environment Controlled Agriculture, Ministry of Agriculture and Rural Affairs, College of Biosystems Engineering and Food Science, Zhejiang University, Hangzhou 310058, China
[b] Department of Agricultural and Environmental Engineering, Faculty of Engineering, Bayero University, Kano, Nigeria
[c] Department of Nutrition & Food Science, National Research Centre, Giza, Dokki, Egypt
[d] Department of Environmental Engineering, School of Architecture and Civil Engineering, Chengdu University, Chengdu 610106, China
[e] Department of Civil and Environmental Engineering, Islamic University of Technology (IUT),Gazipur 1704, Bangladesh

ARTICLE INFO

Editor: Dr. GL Dotto

Keywords:
Recirculating aquaculture system (RAS)
Moving bed biofilm reactor (MBBR)
Mature biofilms
Nitrite removal
Aerobic denitrifiers
Partial least squares-discriminant analysis (PLS-DA)

ABSTRACT

Innovative removal of toxic nitrite and ammonia is one of the key approaches for efficient aquaculture biotechnology. This study suggests a fast removal technique of high-levels of nitrite and ammonia using recirculating aquaculture wastewater at 30‰ salinity. Four lab-scale moving bed biofilm reactors (MBBRs; R1, R2, R3, and R4) were operated in parallel for 56 days with different combinations of mature and fresh biofilms on biocarriers at 30% filling ratio. Nitrogen removal efficiency, biofilm physicochemical properties, and microbial analyses were conducted using PCR and sequencing techniques at the region of the 16S ribosomal RNA. The results showed that R4 (using mature biofilms) recorded the highest nitrite and ammonia removal (99.6% and 95.3%, respectively) compared to the control, R1 (94.1% and 89.4%). Meanwhile, the removal rate of ammonia in R4 was significantly the fastest compared to other reactors. Partial Least Squares-Discriminant Multivariate Analysis (PLS-DA) model showed a good prediction with very high accuracy and prediction ($Q2 > 0.8$) for the first three principal components pertaining to nitrite and ammonia removal. *Planktosalinus* genus was the most abundant in R4, while proteobacteria phylum was the dominant, followed by *Marinobacter* and *Nitrospina* in all reactors. Overall, the use of mature biofilms in MBBR was proven to increase bacterial diversity, enhancing nitrite and ammonia removal efficiency.

1. Introduction

Recently, the recirculating aquaculture system (RAS) is getting fast growth worldwide due to its stable and excellent performance for fish production and proper control of undesired pollutants. It is estimated that aquaculture would account for 62% of the world's fish supply for human consumption by 2030 [1]. However, RAS faces high levels of nitrite and ammonia produced in the bioreactors and especially challenging for saline aquaculture systems. Aquatic organisms, in general, adapted to relatively low levels of nitrite and ammonia concentrations. Thus, high nitrite and ammonia levels hinder marine animals' ability to grow and reproduce [2]. In natural water bodies, nitrite concentration is usually below 0.07 mg L^{-1}, though it can exceed 50 mg L^{-1} in intensive aquaculture systems [3], which accumulates due to the oxidation metabolism of ammonia and due to imbalances in the activity of nitrifying bacteria [4]. Nitrate usually has much lower toxicity when compared to nitrite and ammonia and can be kept low by ensuring timely and proper water exchange in intensive aquaculture systems [2].

The toxic effect of nitrite disrupts multiple physiological functions in fishes, including cardiovascular, ion-regulatory and respiratory, endocrine, and excretory processes [5–7]. A high level of nitrite also hinders the transportation of oxygen in the bloodstream of aquatic organisms, thereby oxidizing hemoglobin to methaemoglobin [8,9]. In a study conducted by Dutra et al. [10], 100% mortality rate was recorded in the freshwater prawn *Macrobrachium amazonicum* within 24 h at 4–16 mg L^{-1} nitrite level, while a lower level of nitrite (2 mg L^{-1}) recorded a mortality rate of 40% during 96 h. The study confirmed nitrite toxicity even at the lower concentration of 1 mg L^{-1}, resulting in a mortality rate

* Corresponding author.
E-mail address: dezhaoliu@zju.edu.cn (D. Liu).

https://doi.org/10.1016/j.jece.2021.105947
Received 14 March 2021; Received in revised form 17 June 2021; Accepted 25 June 2021
Available online 29 June 2021

of 27% during 96 h. Additionally, Barbieri et al. [11] reported an increase in ammonia excretion and oxygen consumption from the white shrimp *Litopenaeus schmitti* exposed to nitrite and low salinity, even though this species is relatively resistant to the environmental nitrite.

The oxidation of nitrite to nitrate by the nitrite-oxidizing microbes was the second of the two-stages of nitrification process [12]. However, a delay in converting nitrite to nitrate results in an elevation of nitrite in water bodies, raising its toxicity level, especially on the fish species. Furthermore, an imbalance between the populations of ammonia-oxidizing bacteria (AOB; like *Nitrosomonas*) and nitrite-oxidizing bacteria (NOB; like *Nitrobacter*) can lead to high levels of nitrite within the first 4–8 weeks of biofilter start-up as a result of the insufficient surface area of dissolved oxygen [13–15]. Furthermore, nitrification deficiency might be due to the lower nitrite oxidizers' growth rate than ammonia oxidizers. Such a problem is usually maintained through *Nitrosomonas* and *Nitrobacter* percentages balancing in the aquaculture systems [16]. Among the various methods that are currently in use for the treatment of wastewater, biological treatment methods are preferred the most due to many advantages over other techniques, such as its low operational cost, low potential toxicity, low energy consumption, chemical-free, environmentally-friendly, and higher nutrients removal efficiency [17–19].

Maintaining healthy biomass on the biofilter surface is directly proportional to its successful usage. Therefore, to maintain healthy, steady, and active biomass, a constant supply of required nutrients is needed, facilitating the three major biological processes happening on a biofilter, including attachment, growth, and decay/detachment of microbes from biocarriers [20]. In an experiment conducted by Hoang et al. [21], the nitrification rates, biomass viability, morphology of nitrifying biofilms, and bacterial community responses from young and mature biofilms in MBBRs were investigated. The study found that mature biofilm becomes significantly thicker, darker in color, and has a higher removal rate than young biofilms. As for the full maturity period of biofilms, the OECD guidelines for the aerobic sewage treatment reported that at least 14 weeks are required to develop a mature biofilm with an additional 4–8 weeks after introducing the test surfactant before acclimatization [22]. Also, Wang et al. [20] reported that it might take up to 17 weeks to complete the process of biofilm development fully.

MBBR technology is globally accepted as a biological treatment method to treat RAS wastewater, especially in addressing nitrogenous compound pollutants' removal via the nitrification process. However, one of the disadvantages of biological treatment methods is the lengthy start-up period, hence establishing new and faster methods is essential from commercial and practical aspects. To the best of the authors' knowledge, no research has so far evaluated the impact of mature biofilm at varying ratios with new biocarriers and nitrifier inoculation on the high-level toxic nitrite and ammonia in biofilm reactors. Therefore, this study aimed to conduct a test to enhance the fast removal of high-level toxic nitrite and ammonia using MBBR technology with varying combinations of mature and fresh biofilms on biocarriers and with nitrifier inoculation. The optimization of the experimental conditions, mainly bacterial inoculation and biofilms carrier mixing ratio, was performed. Besides, the morphology of the biofilms was examined using a scanning electron microscope (SEM). Moreover, the bacterial community composition and relative abundance were evaluated using 16S rRNA pyrosequencing.

2. Materials and methods

2.1. Experimental set-up

The four identical cylindrical reactors used in this study were made from Poly(methyl methacrylate) with 190 mm inner diameter, 400 mm height, and 10 L working volume. The reactors were filled with high-density polyethylene (HDPE) biocarriers (type K5, AnoxKaldnes™) with a bulk specific surface area of 800 $m^2\ m^{-3}$, a height of 3 mm, a diameter of 25 mm, a density of 0.96 g cm^{-3}, and porosity of 75%. An overall biocarrier filling ratio (FR) of 30% ($V_{biocarriers}V^{-1}_{reactor}$) was adopted, providing a surface area of 2.4 m^2 for the biofilm attachment in each reactor as previously suggested [16,23]. Fig. 1 shows the schematic diagram of the four reactors used and the experimental set-up, with the details of the reactors' configurations discussed in Section 2.2. The four reactors ran continuously, and the simulated influent RAS wastewater changed every 24 h. Throughout this study, the dissolved oxygen (DO) level was well monitored and maintained at >5.5 mg L^{-1} using an 80 W air compressor (ACO-Air pump, Sensen Group Co., Ltd., China) fitted with air-stones at the bottom of the reactors for both oxygen supply to the microbial mass and for mixing of biocarriers. The pH level was maintained at 7.5 ± 0.25 using $NaHCO_3$ both as a pH stabilizer and a source of inorganic carbon for bacterial growth, which results in recording a chemical oxygen demand (COD) of 12–18 mg L^{-1} [24]. The whole experiment was kept in a thermostatic chamber at 25–28 °C throughout the study period.

2.2. Reactor configurations

The first reactor (R1) was filled with new biocarriers without nitrifier inoculation as a control reactor to detect the possible bacterial cross-contamination [25]. The second reactor (R2) contained new biocarriers with 0.05 g L^{-1} of aerobic nitrifier inoculant (Huihai Environmental Protection Technology Co., Jiangxi, China), following the manufacturer's guidelines. The R2 content was acclimatized for seven days with full aeration before setting other reactors [23]. The third reactor (R3) contained $^2/_3$ new biocarriers and $^1/_3$ of biocarriers with mature nitrifying biofilms firmly attached to their surfaces. Finally, the fourth reactor (R4) had biocarriers with mature nitrifying biofilms attached to their surfaces. The biocarriers with mature biofilms used in R3 (only $^1/_3$ of the total biocarrier FR) and those used in R4 were obtained from a stable RAS that uses MBBR technology and operates for 18 months in Zhejiang University (Hangzhou, China). The effluent wastewater was tested every other day, while the influent parameters were measured weekly, all in triplicates. The experiments were performed for 56 days, then biocarrier samples were collected from each reactor and immediately stored in sterile 50 mL plastic tubes at −20 °C for further microbial community analysis.

2.3. Characteristics of simulated saline RAS wastewater

The simulated saline RAS wastewater medium used in the present study was adopted from previous studies [16,26], with slight modifications. It was composed of (per 10 L) 0.191 g NH_4Cl (5 mg NH_4^+ −N L^{-1}), 0.986 g $NaNO_2$ (20 mg NO_2^- −N L^{-1}), 3.036 g $NaNO_3$ (50 mg NO_3^- −N L^{-1}), 0.1 g $MgSO_4.7\ H_2O$, 0.22 g K_2HPO_4, 0.2 g $CaCl_2$, 10 g $NaHCO_3$, 1 g $Na_2HPO_4.12\ H_2O$, and 300 g NaCl. This simulated RAS wastewater with a salinity of 30‰ was then continuously fed into the MBBRs from the bottom using a peristaltic pump (BT100–2J, Baoding Longer Precision Pump Co., Ltd., China) at 2.3 rpm for a 24 h HRT throughout the study. All the reagents used in the study were of analytical grade.

2.4. Chemical analyses and performance evaluation

Grab water samples from the influent and effluent were periodically taken, filtered through a 0.45 μm pore size membrane filter, and analyzed for pH (STARTER3100, OHAUS, USA), DO (STARTER300D, OHAUS, USA), nitrite-N (NO_2^- − N), nitrate-N (NO_3^- − N), and ammonia-N (NH_4^+ −N) using a UV-Vis spectrophotometer (Cary-60, Agilent Technologies, Australia) according to standard operating procedures [27]. Reactors' performances were evaluated by monitoring the removal efficiencies of NO_2^- −N and NH_4^+ −N in the system. The NO_3^- −N accumulation of the whole system was also analyzed from each of the

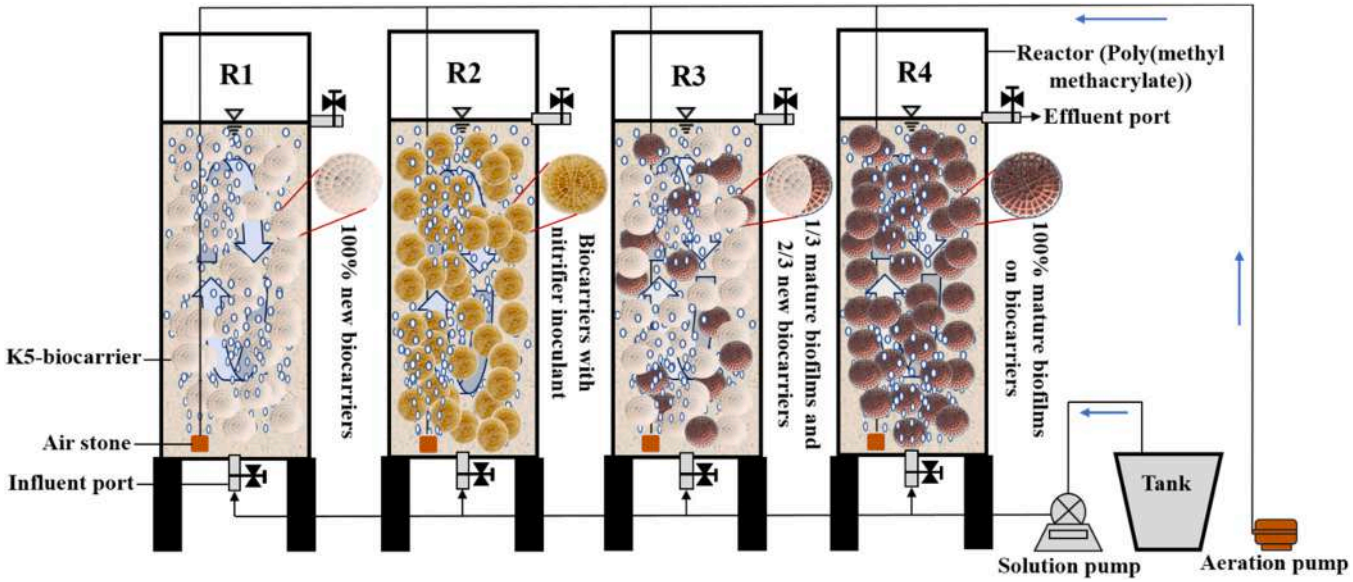

Fig. 1. Schematic diagram showing the experimental set-up using four moving bed biofilm reactors (R1-R4).

reactors. All tests were conducted in triplicates. Therefore, the overall nitrogen conversion activities were observed, quantified, and reported during the entire experimental period.

2.5. Microbial community analysis

2.5.1. DNA extraction and PCR amplification

Biofilm carrier samples were collected in triplicates from the reactors at the end of the study (Day 56). After detaching the biomass from the biocarriers, QIAamp DNA mini kit was used to extract the DNA from the biomass according to our previous work [26] and stored at − 20 °C until use. Briefly, the primers 341F 5′-CCTAYGGGRBGCASCAG-3′ and 806R 5′-GGACTACNNGGGTATCTAAT-3′ were used to amplify the V3-V4 hypervariable region of the 1S rRNA. The thermal cycling included an initial denaturation step of 2 min at 95 °C, followed by 25 cycles for denaturation at 95 °C for 30 s, annealing at 55 °C for 30 s, extension at 72 °C for 30 s, and a final extension step of 5 min at 72 °C using PCR (Phusion High-Fidelity PCR Maser Mix, New England Biolabs). Purified PCR products were sequenced on the Ion S5TM XL platform by BGI Genomics Co. (Hangzhou, China), and single-end reads were generated at 400–600 bp^{-1} for supplementary analysis of the generated data.

2.5.2. Illumina MiSeq sequencing and data processing

AxyPrep DNA Gel Extraction Kit (Axygen-Biosciences, USA) was used in purifying the extracted amplicons from 2% agarose gels. The purified amplicons were then sequenced on a MiSeq platform (Illumina, CA, USA) using a MiSeq Reagent kit V3. The obtained raw fastq files were quality-filtered using QIIME (version 1.17). The clustered operational taxonomic units (OTUs) with 97% similarity were cut-off by UPARSE (version 7.1, http://drive5.com/uparse/) and analyzed by RDP Classifier (http://rdp.cme.msu.edu/) against the Silva (SSU115) 16S rRNA database with the confidence threshold of 70%.

2.6. Biofilm morphology analysis using SEM

SEM (Phenom ProX, Netherland) was used to check the bacterial morphology in the formed biofilm. The biocarrier sample was prepared according to Zheng et al. [28] with some modifications. First, the sample was centrifuged at 5000 rpm for 10 min at 4 °C, then washed twice with 0.85% saline and fixed with 3% glutaraldehyde buffer overnight. After which, it was re-washed three times using 0.1 M phosphate buffers (pH 7.0). Samples were then dehydrated using graded ethanol series (50%, 60%, 70%, 80%, 90%, and 100%) for 15 min each, then freeze-dried. Finally, the samples were placed on an aluminum stub, sputtered with gold, and then examined using SEM at 15 kV.

2.7. Statistical analysis

The SPSS software (version 25, IBM Corporation, USA) was employed for statistical analysis. Graphs were plotted using OriginPro 2017 software (OriginLab Corporation, USA). Results obtained were analyzed using one-way analysis of variance (ANOVA) followed by Duncan's New Multiple Range Test at probability level (P) < 0.05. Also, metaboanalyst software (MetaboAnalystR, CA) was employed for descriptive and predictive modeling of the responses obtained from the reactors using partial least squares-discriminant multivariate analysis (PLS-DA) [29].

3. Results and discussion

3.1. Performance of the reactors

3.1.1. Ammonia removal

The influent NH_4^+ −N concentration in all reactors was maintained at around 5 mg L^{-1} during the whole experiment (Fig. 2a). The NH_4^+ −N concentration in R2 slightly increased to 5.6 mg L^{-1} immediately (Day 2), then dropped to 5.4 mg L^{-1} (Day 4) and continued within this range until day 12, as clearly indicated by the heatmap (Fig. 2b). The rise and fall in NH_4^+ −N concentration in R2 might be attributed to the start-up activity exhibited by the new nitrifier biofilm added in the MBBR. In that context, Li et al. [23] reported that NH_4^+ −N effluent of MBBR has fluctuated after 16 days of starting their experiment based on the added amount of the nitrifying bacteria inoculants. Further, the NH_4^+ −N concentration in R2 continued to drop until day 40, reaching zero, where a similar trend was also observed in the other reactors. After day 40, NH_4^+ −N concentration in all the reactors continued stabilizing up to day 56, recording a value <1 mg NH_4^+ −N L^{-1}, with a similar stability pattern that was by Gonzalez-Silva et al. [16], in which different salinity content was nevertheless used than that in this study.

Furthermore, it was observed in R1 and R3 that the NH_4^+ −N concentration exhibited a comparable pattern from the beginning until day 12, decreasing to 3.5 mg L^{-1} and 3.7 mg L^{-1} on the 12th day, respectively. Also, a drastic decline in NH_4^+ −N concentration was observed

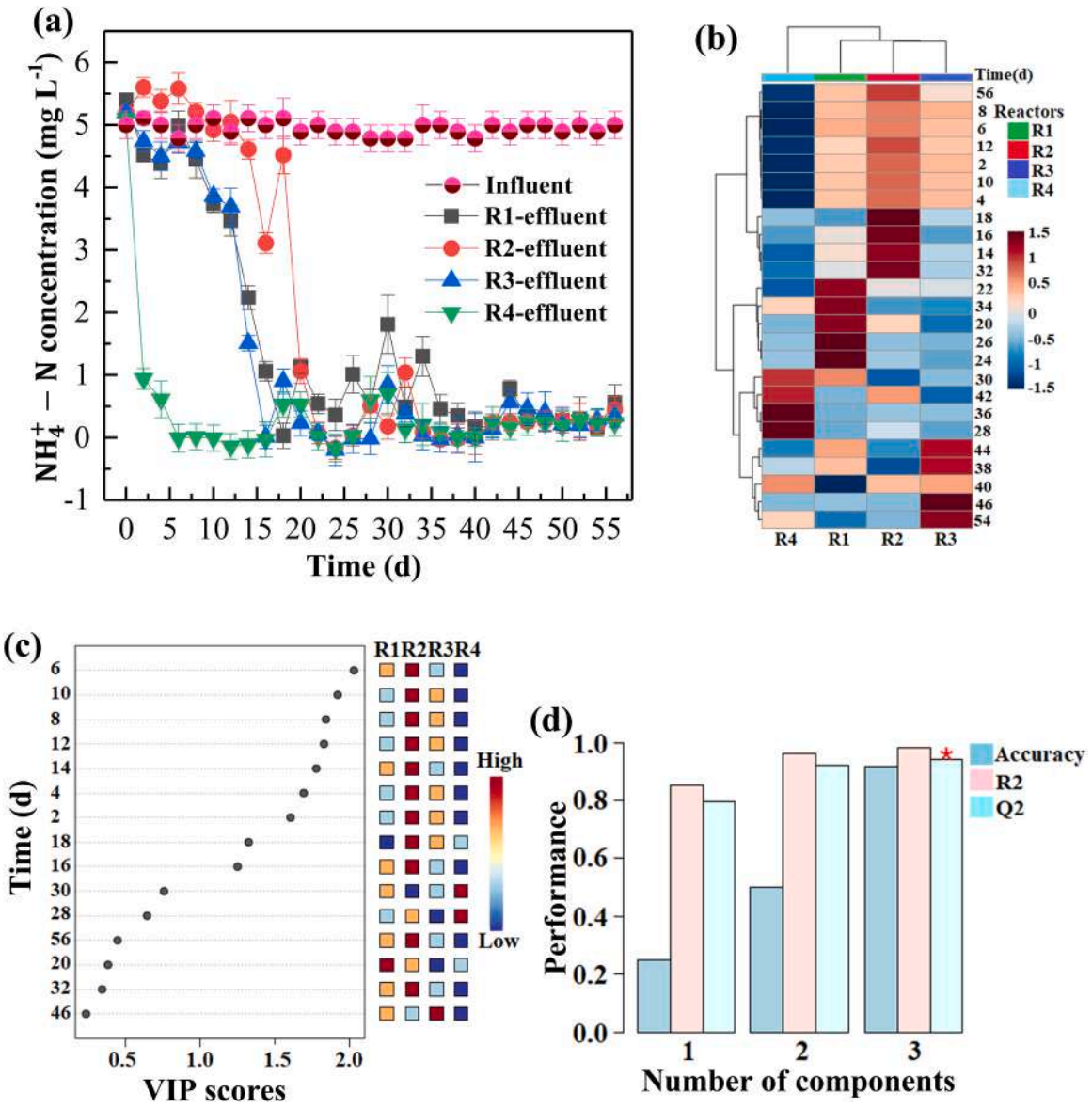

Fig. 2. Ammonia-nitrogen concentration, differentiation, and correlation in the four studied reactors; R1 – contains 100% new biocarriers (control), R2 – contains new biocarriers with nitrifier inoculant, R3 – contains $^1/_3$ biocarriers with mature biofilms and $^2/_3$ new biocarriers, R4 – contains 100% biocarriers with mature biofilms; (a) Ammonia-nitrogen concentration responses from the studied reactors; (b) Clustering results shown as heatmap; (c) The important features identity (VIP) classification by PLS-DA, the colored boxes on the right indicate the relative NH_4^+ –N concentration in each reactor; and (d) Cross-validation (CV) for classification performance with a different number of components based on PLS-DA.

from day 13–40 in both R1 and R3, as shown in Fig. 2a. After that, the NH_4^+ –N concentration in all the MBBRs remained relatively the same until day 56. The behavior exhibited by R1 could be a result of possible bacterial cross-contamination. In that context, Krustok et al. [25] reported the presence of algae-bacteria consortia in sterilized experiments due to cross-contamination from the neighboring reactors during their study. Besides, NH_4^+ –N removal efficiencies of 89.4%, 90.2%, and 91.6% were achieved at the steady-state in R1, R2, and R3, respectively.

For R4 with an already established biofilm, the NH_4^+ –N concentration immediately reduced to less than 1 mg NH_4^+ –N L^{-1} on the second day of commencing the experiment, which has shown an average removal efficiency of 95.3% at the steady-state (Fig. 2a and b). Hence, this indicated the viability of R4 to remove NH_4^+ –N faster than the other MBBRs (R1, R2, and R3) due to the possession of already mature biofilms. It can be seen from Fig. 2b that R4 had the least NH_4^+ –N concentration from the beginning of the experiment until day 12 ($P < 0.05$). Furthermore, the PLS-DA model (Fig. 2c) showed that R4 had the least NH_4^+ –N concentration compared to other reactors. An added advantage of using the model is that it depends not only on the data sets used for the analysis but also on the diagnostic statistic values used to optimize and assess the PLS-DA model's performance in the study [30]. It was demonstrated in a study conducted by Liu et al. [26] that mature biofilms can improve nitrification efficiency. However, from Fig. 2c on days 28 and 30, R4 experienced a relatively low increase in NH_4^+ –N concentration (<0.8 mg L^{-1}) due to a decrease in pH level (it was addressed immediately) below the optimum pH nitrification range (7.2–7.8). Moreover, the pH drop in R4 could be related to the presence of microbes in denser flocs than in other reactors (Fig. 6d), resulting in lower pH at the cell surfaces than the bulk pH of the reactor due to H^+ ions production [31]. Fig. 2d presents the accuracy, cross-validation (CV), and prediction (Q2) based on the optimal number of components determined by PLS-DA. Szymańska et al. [30] reported that Q2 > 0.5 can be considered as proof of the high predictive ability of the PLS-DA

model. The model showed a good prediction with very high accuracy and Q2 > 0.8 (Fig. 2d) for the first three principal components (PCs).

Nonetheless, towards the tail end of this study, all the MBBRs exhibited almost similar kinetics concerning NH_4^+ −N removal despite having a different set-up. Also, the variations in the MBBRs' performances, especially from day 1–12, could be directly linked to the difference in the quantity and bioactivity of the functional microorganisms present in the MBBRs [32]. Also, *Bacteroidetes* phyla were reported to possess a highly stable ability to remove ammonia and chemical oxygen demand (COD) under aerobic conditions [23]. Thus, it can be deduced from the responses observed in the MBBRs that using mature biofilms on biocarriers offers a faster and more promising result in biologically operated systems. Correspondingly, the higher the number of viable microbes in the bioreactors, the better, faster, and higher ammonia removal achieved.

3.1.2. Nitrite removal

The influent NO_2^- −N concentration in all the reactors was maintained at around 20 mg L^{-1} (Fig. 3a). R1 and R2 followed a similar trend from day 1–12, where NO_2^- −N decreased to 11.7 mg L^{-1} and 11.5 mg L^{-1} (Day 2), then increased to 21.8 mg L^{-1} and 18.6 mg L^{-1} on day 12, respectively. However, from day 12–40, R1 and R2 showed significant differences in NO_2^- −N ($P < 0.05$), where it decreased sharply in R2, reaching 2.4 mg L^{-1} on day 40, while R1 showed a significant increase up to 27.6 mg L^{-1} on day 22, then reduced to 6.5 mg L^{-1} on day 40 (Fig. 3a and b). Differently, R3 and R4 showed a continuous reduction in NO_2^- − N, reaching the minimum value of around 1.2 mg L^{-1} and 0.3 mg L^{-1} on day 18, respectively, followed by stability until the end of the experiment (Day 56).

The succession increases and decreases of NO_2^- −N concentration witnessed in R1 from day 12–40 might be attributed to the nature of the reactor contents being fresh initially, then changed due to possible bacterial cross-contamination [25]. Similarly, such fluctuations in NO_2^- −N concentration, if not well monitored and kept under control, could lead to serious negative consequences on the biofilter performance [33], which may eventually lead to high mortality of aquatic species [5]. During the biological nitrification process, TAN oxidation is executed first, before the NO_2^- −N oxidation, hence the NO_2^- −N accumulation could occur [33]. To control such fluctuation and accumulation of NO_2^- − N, factors like inorganic-N concentrations, temperature, pH,

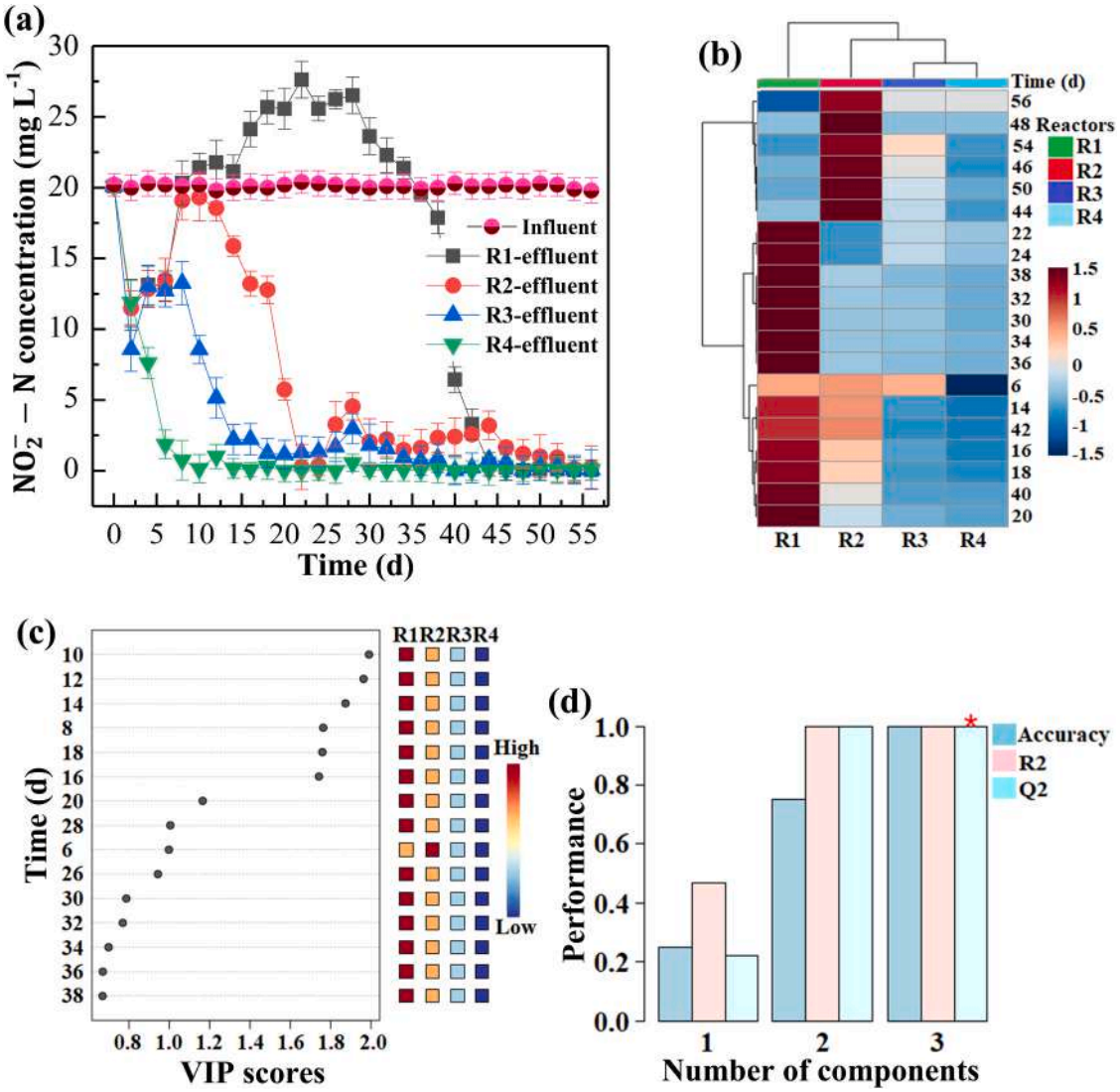

Fig. 3. Nitrite-nitrogen concentration, differentiation, and correlation in the four studied reactors: R1 – contains 100% new biocarriers (control), R2 – contains new biocarriers with nitrifier inoculant, R3 – contains $^1/_3$ biocarriers with mature biofilms and $^2/_3$ new biocarriers, R4 – contains 100% biocarriers with mature biofilms; (a) Nitrite-nitrogen concentration responses from the studied reactors; (b) Clustering results shown as heatmap; (c) The important features identity (VIP) classification by PLS-DA, the colored boxes on the right indicate the relative NO_2^- −N concentration in each reactor; and (d) Cross-validation (CV) for classification performance with a different number of components based on PLS-DA.

aeration, and balancing of AOB and NOB should be closely monitored and balanced [34].

Furthermore, the NO_2^- −N concentration in R2 finally stabilized to 0.3 mg L^{-1} on day 56 with an average removal efficiency of 97.1% (Fig. 3a). Similarly, R1 stabilized to 0.1 mg L^{-1} with a removal efficiency of 94.1% within the detection limit. However, for R3 and R4, a drastic decrease from day 1–12 was recorded as 5.1 mg L^{-1} and 1.0 mg L^{-1}, respectively. Meanwhile, R3 and R4 continued in the same pattern through days 14–56. However, R4 showed a slightly higher removal efficiency of 99.6% than R3 (98.6%), as depicted in Fig. 3a and c. Thus, the results obtained from R3 and R4 confirmed the mature biofilms' ability to hasten the removal of NO_2^- −N from RAS wastewater compared to fresh inoculation of AOB used in R2. Also, the difference in performance between the studied reactors has been depicted in Fig. 3c using color coding, with R4 having the least concentration of NO_2^- −N and highest performance based on Variable Importance in Projection (VIP scores), followed by R3, R2, and finally R1 (control). Moreover, the system's accuracy based on the PLS-DA model showed Q2 > 0.97 for the second and third PCs (Fig. 3d). The differences in NO_2^- −N removal performances were attributed to the biofilm characteristics and the bacterial diversity in the four reactors [32] due to different bacterial inoculation strategies applied in each reactor (Fig. 5(b,c) and Fig. S1). Additionally, it was clear that nitrite oxidation was successful in all MBBRs as NO_2^- −N concentrations remained low (<0.25 mg NO_2^- −N L^{-1}) during the steady-state (Day 40–56), as shown in Table 1.

3.1.3. Nitrate accumulation

The influent NO_3^- −N concentration was adjusted to around 50 mg L^{-1} in the four studied reactors (Fig. 4a). Reactors R1, R2, and R3 showed a slight decrease in effluent NO_3^- −N concentration on day 2, then increased up to 51.8, 52.4, and 67.0 mg L^{-1}, respectively, on day 12. However, R4 showed a gradual increase in NO_3^- −N concentration, which rose immediately to 51.7 mg L^{-1} on day 2, then increased gradually to 75.6 mg L^{-1} on day 12. The steep increase of NO_3^- −N in R4 (51.7 mg L^{-1} to 75.6 mg L^{-1}) might be due to the established native nitrifying biofilms on the biocarriers used. This faster response in terms of NO_3^- −N accumulation in R4 can also be confirmed by both the heatmap (Fig. 4b) and the PLS-DA model (Fig. 4c).

From day 12, all the reactors continued with NO_3^- −N accumulation at different rates until day 40, where almost similar rates were recorded (Fig. 4a). Although R1 (control) demonstrated a slight deviation from other reactors with a slow increase from day 12–38, it rose steeply to 70.8 mg L^{-1} on day 40. This behavior exhibited by R1 might be due to the reactor contents being fresh at the beginning, then contaminated later as a result of possible microbial cross-contamination [25]. In the stabilization stage (Day 40–56), a similar trend was observed for all the reactors, with an average NO_3^- −N accumulation of 54.7 ± 3.5%. Gradual NO_3^- −N increase was recorded due to NO_2^- −N and NH_4^+ −N removal in the reactors as a result of sufficient aeration that resulted in zero denitrification [35]. Also, the NO_3^- −N accumulation was found to have a very high accuracy based on the PLS-DA model indicators for the second and third PCs (Q > 0.97) (Fig. 4d). It is worth noting that NO_3^- −N concentration that keeps accumulating up to the end of this study (Day 56) resulted from continuously operating the MBBRs without freshwater exchange, as equally reported by Stavrakidis-Zachou et al. [36].

The effluent nitrate fluctuation resulted from the production of nitrate being the second stage of the two-stage pathway of the nitrification process; hence, nitrate accumulation usually records less consistency than ammonia and nitrite both before and while the steady-state [23]. Nitrate fluctuation might also be due to partial denitrification within the system due to the availability of microbial biomass, which serves as a carbon source to aerobic-denitrifiers like *Pseudomonas* [37,38] identified in this study (Figs. 5c and S1). Hence, achieving nitrate accumulation and stabilization is a complex process under aerobic conditions [39].

3.2. Microbial community analysis

3.2.1. Composition and relative abundance of microbial community structure

The biofilm communities of the four nitrifying MBBRs were characterized by pyrosequencing of 16S rRNA amplicons. Operational taxonomic units (OTUs) obtained for R1, R2, R3, and R4 were 228, 204, 211, and 271, respectively (Table 2). Fig. 5a shows a Venn diagram that evaluates the unique and shared OTUs of the nitrifying bacterial communities present in the studied reactors. It can be noted that the highest proportion of 17.1% (156 OTUs) was shared between all reactors. R1, R3, and R4 commonly shared 20 OTUs (2.2%), followed by R1, R2, and R4, with 14 common OTUs (1.5%). The lowest percentage of the shared OTUs was found between R1 and R2 (0.2%), with only two common OTUs. Besides, the highest percentage of unique OTUs was found in R4 (4.2%), followed by R2 (1.0%) then R1 (0.8%). R4, having the highest number of OTUs (271), was also observed to contain the highest alpha-diversity indices in Shannon, Simpson, Chao1, and Abundant Chao Estimates (ACE), as shown in Table 2. These observations indicate that the richest bacterial community abundance was in the reactor containing mature biofilms (R4). Moreover, the lowest percentage of unique OTUs was found in the reactor containing $^2/_3$ new biocarriers and $^1/_3$ of the established native nitrifying biofilms (R3). Hence, 6.6% of the total OTUs were uniquely distributed in the four reactors (Fig. 5a).

Furthermore, the relative abundance of the top-ten dominant phyla of the bacteria in all the reactors was analyzed and presented in Fig. 5b. It was observed at the phylum level (Fig. 5b) that many known bacterial phyla were detected from all the reactors, such as *Proteobacteria, Bacteroidetes, Nitrospinae, Actinobacteria, Firmicutes, Chloroflexi, Verrucomicrobia, Planctomycetes,* and *Chlamydiae*. The discovery of these known phyla in this study (listed in descending order of their abundance) is consistent with a recent study by Gao et al. [40], where they observed a decline in the quantity of these bacterial phyla due to an increase in salinity level. *Proteobacteria* being amongst the microorganisms that enable ammonia oxidation in addition to degradation of organic

Table 1
Effluent-water operating parameters in the MBBRs at steady-state (Day 40–56).

Parameter	**Value***				**Unit**
Temperature	25–28				°C
DO	>5.50				mg L^{-1}
pH	7.50 ± 0.25				–
Salinity	30				‰
COD	12–18				mg L^{-1}
Reactor codes	**R1**	**R2**	**R3**	**R4**	**Unit**
NH_4^+ − N	0.38 ± 0.14	0.26 ± 0.22	0.28 ± 0.34	0.23 ± 0.07	mg L^{-1}
NO_2^- − N	0.15 ± 0.00	0.20 ± 0.01	0.08 ± 0.01	0.08 ± 0.02	mg L^{-1}
NO_3^- − N	77.41 ± 1.98	78.95 ± 0.50	77.60 ± 1.06	79.72 ± 0.12	mg L^{-1}

* Mean ± SD values, DO – dissolved oxygen, COD – chemical oxygen demand, R1 – control, R2 – contains nitrifier inoculant, R3 – contains $^1/_3$ biocarriers with mature biofilms and $^2/_3$ new biocarriers, R4 – contains biocarriers with mature biofilms.

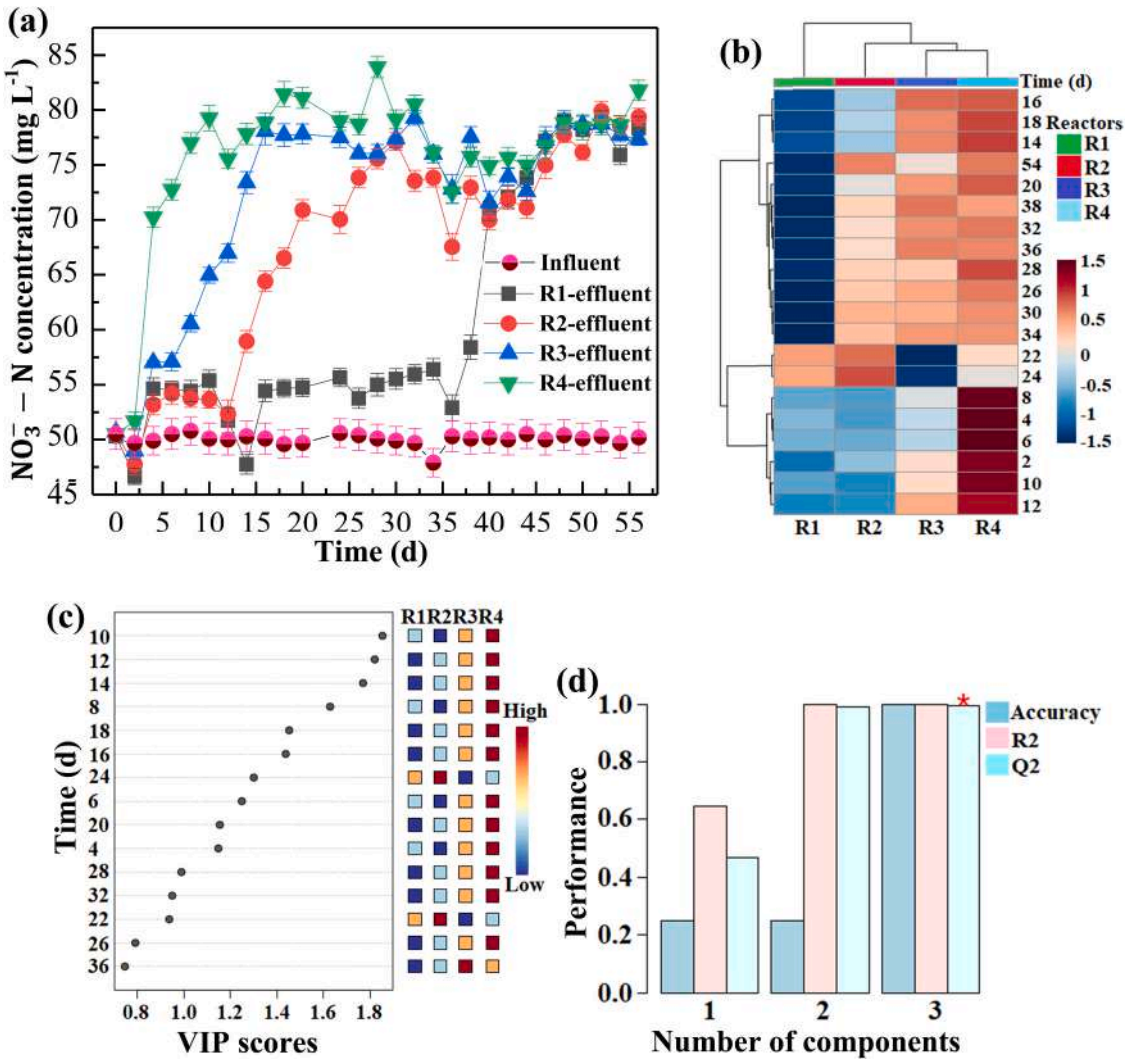

Fig. 4. Nitrate-nitrogen concentration, differentiation, and correlation in the four studied reactors: R1 – contains 100% new biocarriers (control), R2 – contains new biocarriers with nitrifier inoculant, R3 – contains $^1/_3$ biocarriers with mature biofilms and $^2/_3$ new biocarriers, R4 – contains 100% biocarriers with mature biofilms; (a) Nitrate-nitrogen concentration responses from the studied reactors; (b) Clustering results shown as heatmap; (c) The important features identity (VIP) classification by PLS-DA, the colored boxes on the right indicate the relative NO_3^- –N concentration in each reactor; and (d) Cross-validation (CV) for classification performance with a different number of components based on PLS-DA.

nutrients in wastewater (under aerobic conditions) [41], was found to be the most abundant bacteria with the highest population in R4 (70.44%), followed by R1 (63.50%) then R3 (60.01%), which is in consistence with the result reported by Guan et al. [42]. R2 had the least *Proteobacteria* (48.33%) with the highest population of Bacteroidetes (45.92%) as compared to R1 (29.51%), R3 (28.15%), and R4 (16.57%). The phylum Verrucomicrobia, also discovered in this study, was related to several other bacterial phyla that led to forming a superphylum cluster [43]. This superphylum consists of *Planctomycetes, Verrucomicrobia,* and *Chlamydiae,* commonly called the PVC-superphylum, where *Verrucomicrobia* was specifically known to participate in glucose homeostasis in living cells [43,44]. The investigation further revealed that *Planktosalinus*, *Marinobacter*, and *Nitrospina* were the most abundant potential heterotrophic bacterial genera. Simultaneously, Flavobacteriaceae and Bacteroidia were the most abundant family and class, respectively, in all the reactors.

Moreover, the most abundant genus found in Bacteroidetes was *Plankitosalinus*, depicted in the genus evolutionary tree, showing relative abundance and diversity of microbes in the four studied reactors (Fig. 5c). For the relative abundance of the bacterial order (Fig. S1 in the E-supplementary data), Flavobacteriales was the most abundant in R2 (44.92%) followed by R3 (26.80%) and R1 (26.61%). On the other hand, R4 recorded the least Flavobacteriales (14.67%) while having the highest population of Rhizobiales (18.35%) as compared to R2 (12.45%), R1 (15.97%), and R3 (16.53%). The predominance of *Proteobacteria* phyla in R4 was attributed to the order Rhizobiales of Alphaproteobacteria class, which was also the most abundant bacterial order in R4 [45]. Also, the abundance of *Proteobacteria* and *Bacteroidetes* at the phyla level was in line with the results reported by Chang et al. [46], whereby aeration mode influenced the relative abundance of the aforementioned bacterial phyla community. Moreover, the phyla *Bacteroidetes* is a fermentative bacterium reported to possess a highly stable ability to remove ammonia and chemical oxygen demand (COD) under aerobic conditions [23]. *Bacteroidetes* were also reported to be highly enriched under high aeration intensity than other bacterial phyla [47].

The weighted pair-group method with arithmetic mean (WPGMA) clustering analysis was performed, as shown by the beta-hierarchical dendrogram in Fig. S2a (E-supplementary data), which presented the same result as that of Fig. 5b, showing the relative abundance at the phyla level in the top-ten. The dendrogram results using two distance matrixes (weighted unifrac and unweighted unifrac) were combined with the overall percentages of relative abundance among all samples at

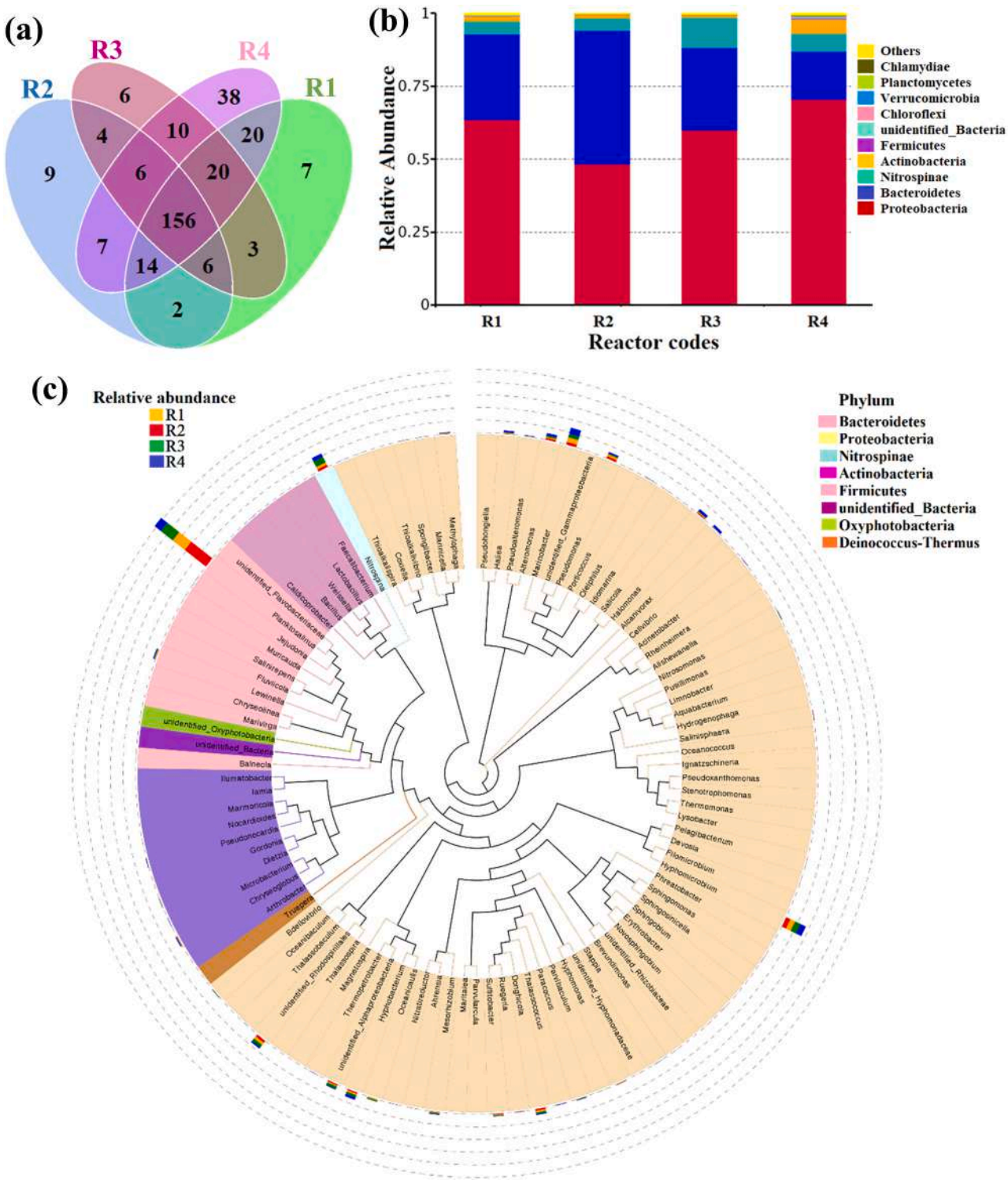

Fig. 5. Venn-diagram showing alpha-diversity of the observed species (a); Relative abundance of the top-ten dominant phyla (b); and the genus evolutionary tree showing relative abundance and diversity of microbes in the four studied reactors (c): R1 – contains 100% new biocarriers (control), R2 – contains new biocarriers with nitrifier inoculant, R3 – contains $^{1}/_{3}$ biocarriers with mature biofilms and $^{2}/_{3}$ new biocarriers, R4 – contains 100% biocarriers with mature biofilms.

the phylum level in the top-ten (Fig. S2a and b). The unweighted unifrac results depicted in Fig. S2b showed that *Proteobacteria* and *Bacteroidetes* were the most abundant bacterial phyla, and were consistent with a previous study on biofilm reactors where a conventional molecular biology method was applied [47]. This finding was revealed by the weighted unifrac (Fig. S2a), with only the third most abundant phyla being *Actinobacteria* in the latter [42]. Besides, the discovery of *Firmicutes* in this study (Fig. 5b), as equally reported by Zhang et al. [41], was among the reasons that ensured stability during the nitrification process, especially at high salinity, as it is capable of producing spores that resist dehydration and other severe environmental conditions.

3.2.2. *Microbial morphology*

The bacterial populations from the biocarrier samples from the

Table 2
Alpha-diversity of the bacterial community from the four studied MBBRs.

Sample name	Observed species	Shannon	Simpson	Chao1	ACE	Good coverage	PD whole tree
R1	228	4.908	0.914	235.308	239.087	1	21.032
R2	204	4.003	0.790	211.600	215.985	1	19.459
R3	211	4.712	0.911	230.500	231.266	0.999	19.918
R4	271	5.632	0.961	284.588	281.969	1	24.011

R1 – control, R2 – contains nitrifier inoculant, R3 – contains $^{1}/_{3}$ biocarriers with mature biofilms and $^{2}/_{3}$ new biocarriers, R4 – contains biocarriers with mature biofilms, ACE – Abundant Chao Estimates, PD – phylogenetic diversity.

studied reactors were analyzed using SEM (Fig. 6). The SEM micrographs shown in Fig. 6a and b represented R1 and R2, respectively, with a morphological homogeneity and relatively smooth surface in the biofilms. Further, Fig. 6c and d representing R3 and R4, respectively, showed homogeneity in their morphology with spines-like structure and high microbial adhesion, thus yielding better nitrification performance. However, in R3, some morphological heterogeneity existed within the bacterial populations, as seen in Fig. 6c, which indicates the accompanying differences in the biofilm cells' physiological states due to combining mature and new biofilms [48]. In R4 (Fig. 6d), there was an absolute morphological homogeneity in the cells' morphological state that forms the biofilms, which confirmed the best performance. Also, the size of biofilm cells in R4 was smaller than those in R3, which might be due to the difference in maturity level, with R4 having more mature biofilms on carriers. The observed diversity in the bacterial morphology indicated by the SEM images is directly associated with the types of the existing bacterial species, as filamentous bacteria were reported to exist and formed flocs under both aerobic and salt conditions [41,49].

4. Conclusion

MBBR with mature biofilms showed an excellent efficiency in removing the high nitrite and ammonia levels within 56 days or less. In the steady state, NO_2^- −N was maintained at a low level (<0.25 mg L^{-1}), signifying that satisfactory nitrite oxidation was achieved. Also, NH_4^+ −N was kept below 0.5 mg L^{-1} in all the reactors. *Planktosalinus*, *Marinobacter,* and *Nitrospina* were the most abundant heterotrophic bacteria in all studied reactors. This study opens a thinking idea for further

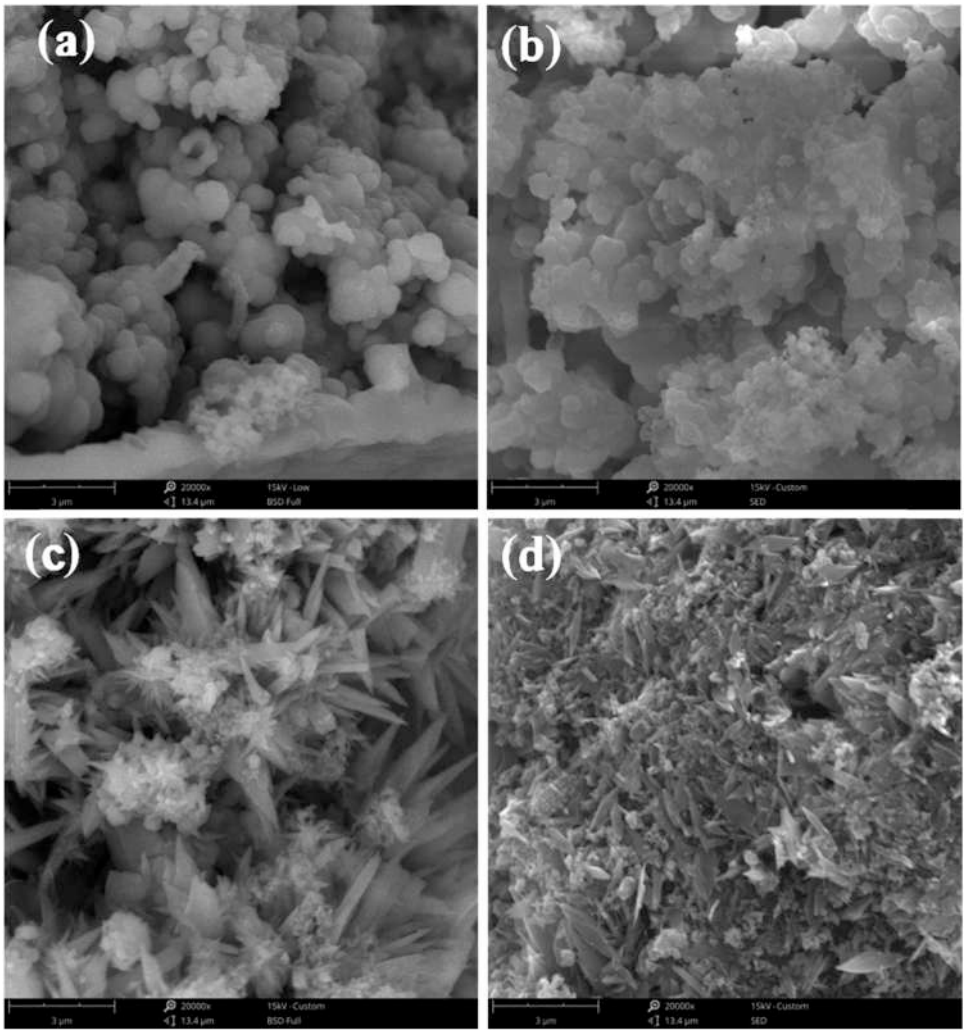

Fig. 6. SEM micrographs of the biofilms on biocarriers in the four studied reactors; (a) contains 100% new biocarriers as control (R1); (b) contains new biocarriers with nitrifier inoculant (R2); (c) contains $^{1}/_{3}$ biocarriers with mature biofilms and $^{2}/_{3}$ new biocarriers (R3); (d) contains 100% biocarriers with mature biofilms (R4).

industrial-scale studies under different salinity conditions, temperature, and pH at a different ratio of new and mature biocarriers, leading to safe re-use and recycling of biocarriers for a greener environment.

CRediT authorship contribution statement

Musa Abubakar Tadda: Conceptualization, Methodology, Investigation, Data curation and analysis, Writing - original draft, Writing - review & editing. **Changwei Li:** Investigation, Writing - review & editing. **Mostafa Gouda:** Data analysis, Writing - review & editing. **Abd El-Fatah Abomohra:** Data analysis, Writing - review & editing. **Abubakar Shitu:** Writing - review & editing. **Amimul Ahsan:** Writing - review & editing. **Songming Zhu:** Resources, Writing - review & editing. **Dezhao Liu:** Conceptualization, Methodology, Supervision, Funding acquisition, Writing - review & editing.

Declaration of Competing Interest

The authors declare that they have no known competing financial interests or personal relationships that could have appeared to influence the work reported in this paper.

Acknowledgements

Support from the Key Research and Development Program of Zhejiang Province (No. 2021C02024; No. 2021C03171) and the Thousand People Project (2016 Youth Thousand Program) are acknowledged. The graduate study was supported by the Two-High Scholarship at Zhejiang University, Hangzhou – China, and is well appreciated and acknowledged.

Appendix A. Supporting information

Supplementary data associated with this article can be found in the online version at doi:10.1016/j.jece.2021.105947.

References

[1] FAO (Food and Agriculture Organization of the United Nations), The State of World Fisheries and Aquaculture 2020, FAO,, Rome, 2020, https://doi.org/10.4060/ca9229en.
[2] J.-H. Kim, Y.J. Kang, K. Il Kim, S.K. Kim, J.-H. Kim, Toxic effects of nitrogenous compounds (ammonia, nitrite, and nitrate) on acute toxicity and antioxidant responses of juvenile olive flounder, Paralichthys olivaceus, Environ. Toxicol. Pharmacol. 67 (2019) 73–78, https://doi.org/10.1016/j.etap.2019.02.001.
[3] J. Wang, H. Tang, X. Zhang, X. Xue, X. Zhu, Y. Chen, Z. Yang, Mitigation of nitrite toxicity by increased salinity is associated with multiple physiological responses: a case study using an economically important model species, the juvenile obscure puffer (Takifugu obscurus), Environ. Pollut. 232 (2018) 137–145, https://doi.org/10.1016/j.envpol.2017.09.026.
[4] L. Yun, Z. Yu, Y. Li, P. Luo, X. Jiang, Y. Tian, X. Ding, Ammonia nitrogen and nitrite removal by a heterotrophic Sphingomonas sp. strain LPN080 and its potential application in aquaculture, Aquaculture 500 (2019) 477–484, https://doi.org/10.1016/J.AQUACULTURE.2018.10.054.
[5] Y.J. Ruan, X.S. Guo, Z.Y. Ye, Y. Liu, S.M. Zhu, Bacterial community analysis of different sections of a biofilter in a full-scale marine recirculating aquaculture system, N. Am. J. Aquac. 77 (2015) 318–326, https://doi.org/10.1080/15222055.2015.1017128.
[6] X.-Q. Gao, F. Fei, H.H. Huo, B. Huang, X.S. Meng, T. Zhang, B.-L. Liu, Effect of acute exposure to nitrite on physiological parameters, oxidative stress, and apoptosis in Takifugu rubripes, Ecotoxicol. Environ. Saf. 188 (2020), 109878, https://doi.org/10.1016/j.ecoenv.2019.109878.
[7] D.T.T. Huong, L.T.H. Gam, S. Lek, V.N. Ut, N.T. Phuong, Effects of nitrite at different temperatures on physiological parameters and growth in clown knifefish (Chitala ornata, Gray 1831), Aquaculture 521 (2020), 735060, https://doi.org/10.1016/j.aquaculture.2020.735060.
[8] J. Ramírez-Rochín, M.G. Frías-Espericueta, J.F. Fierro-Sañudo, S.G. Alarcón-Silvas, M.G. Fregoso-López, F. Páez-Osuna, Acute toxicity of nitrite on white shrimp Litopenaeus vannamei (Boone) juveniles in low-salinity water, Aquac. Res. 48 (2017) 2337–2343, https://doi.org/10.1111/are.13069.
[9] K.H. Kroupová, O. Valentová, Z. Svobodová, P. Šauer, J. Máchová, Toxic effects of nitrite on freshwater organisms: a review, Rev. Aquac. 10 (2018) 525–542, https://doi.org/10.1111/raq.12184.
[10] F.M. Dutra, M. Rönnau, D. Sponchiado, S.C. Forneck, C.A. Freire, E.L.C. Ballester, Histological alterations in gills of Macrobrachium amazonicum juveniles exposed to ammonia and nitrite, Aquat. Toxicol. 187 (2017) 115–123, https://doi.org/10.1016/j.aquatox.2017.04.003.
[11] E. Barbieri, A.C.V. Bondioli, C.B. de Melo, M.B. Henriques, Nitrite toxicity to Litopenaeus schmitti (Burkenroad, 1936, Crustacea) at different salinity levels, Aquac. Res. 47 (2016) 1260–1268, https://doi.org/10.1111/are.12583.
[12] L. Ouyang, B. Thamdrup, M. Trimmer, Coupled nitrification and N_2 gas production as a cryptic process in oxic riverbeds, Nat. Commun. 12 (2021) 1217, https://doi.org/10.1038/s41467-021-21400-3.
[13] Y. Hu, X. Zhao, Y. Zhao, Achieving high-rate autotrophic nitrogen removal via Canon process in a modified single bed tidal flow constructed wetland, Chem. Eng. J. 237 (2014) 329–335, https://doi.org/10.1016/j.cej.2013.10.033.
[14] B. Liu, H. Ren, M. Terashima, N.T. Ha, L.E. Van Chieu, R. Goel. Poisoning and growth inhibition of nitrite oxidising organisms, in: IWA-2017. Sustainable Wastewater Treatment and Resource Recovery: Research, Planning, Design and Operations, Chongqing, China 2017, pp. 1–11.
[15] J.M. Ebeling, Biofiltration-Nitrification Design Overview, New Orleans, L.A, 2018.
[16] B.M. Gonzalez-Silva, K.R. Jonassen, I. Bakke, K. Østgaard, O. Vadstein, Nitrification at different salinities: Biofilm community composition and physiological plasticity, Water Res. 95 (2016) 48–58, https://doi.org/10.1016/j.watres.2016.02.050.
[17] T. Alvarino, S. Suarez, J. Lema, F. Omil, Understanding the sorption and biotransformation of organic micropollutants in innovative biological wastewater treatment technologies, Sci. Total Environ. 615 (2018) 297–306, https://doi.org/10.1016/j.scitotenv.2017.09.278.
[18] C. Hui, X. Guo, P. Sun, R.A. Khan, Q. Zhang, Y. Liang, Y.H. Zhao, Removal of nitrite from aqueous solution by Bacillus amyloliquefaciens biofilm adsorption, Bioresour. Technol. 248 (2018) 146–152, https://doi.org/10.1016/j.biortech.2017.06.176.
[19] E.M. John, K. Krishnapriya, T.V. Sankar, Treatment of ammonia and nitrite in aquaculture wastewater by an assembled bacterial consortium, Aquaculture 526 (2020), 735390, https://doi.org/10.1016/j.aquaculture.2020.735390.
[20] J. Wang, Q. Liu, B. Wu, F. Zhao, S. Ma, H. Hu, X. Zhang, H. Ren, Quorum sensing signaling distribution during the development of full-scale municipal wastewater treatment biofilms, Sci. Total Environ. 685 (2019) 28–36, https://doi.org/10.1016/j.scitotenv.2019.05.249.
[21] V. Hoang, R. Delatolla, T. Abujamel, W. Mottawea, A. Gadbois, E. Laflamme, A. Stintzi, Nitrifying moving bed biofilm reactor (MBBR) biofilm and biomass response to long term exposure to 1C, Water Res. 49 (2013) 215–224, https://doi.org/10.1016/j.watres.2013.11.018.
[22] OECD, Guideline for the Testing of Chemicals: Aerobic Sewage Treatment - Biofilms (303 B), 2001. (https://doi.org/10.1787/9789264067394-eng).
[23] C. Li, J. Liang, X. Lin, H. Xu, M.A. Tadda, L. Lan, D. Liu, Fast start-up strategies of MBBR for mariculture wastewater treatment, J. Environ. Manag. 248 (2019), 109267, https://doi.org/10.1016/j.jenvman.2019.109267.
[24] M. Dezotti, G. Lippel, J.P. Bassin, Advanced biological processes for wastewater treatment, Adv. Biol. Process. Wastewater Treat. (2018), https://doi.org/10.1007/978-3-319-58835-3.
[25] I. Krustok, M. Odlare, M.A. Shabiimam, J. Truu, M. Truu, T. Ligi, E. Nehrenheim, Characterization of algal and microbial community growth in a wastewater treating batch photo-bioreactor inoculated with lake water, Algal Res. 11 (2015) 421–427, https://doi.org/10.1016/j.algal.2015.02.005.
[26] D. Liu, C. Li, H. Guo, X. Kong, L. Lan, H. Xu, S. Zhu, Z. Ye, Start-up evaluations and biocarriers transfer from a trickling filter to a moving bed bioreactor for synthetic mariculture wastewater treatment, Chemosphere 218 (2019) 696–704, https://doi.org/10.1016/j.chemosphere.2018.11.166.
[27] APHA, AWWA, WEF. Standard Methods for the Examination of Water and Wastewater, 23rd ed., American Public Health Association, American Water Works Association, Water Environment Federation,, Washington, DC., USA, 2017 https://doi.org/10.2105/SMWW.2882.216.
[28] Y. Zheng, Z. Zhao, W. Wu, C. Song, S. Meng, L. Fan, X. Bing, J. Chen, Effects of dietary resveratrol supplementation on hepatic and serum pro-/anti-inflammatory activity in juvenile GIFT tilapia, Oreochromis niloticus, Dev. Comp. Immunol. 73 (2017) 220–228, https://doi.org/10.1016/j.dci.2017.03.030.
[29] L.C. Lee, C.Y. Liong, A.A. Jemain, Partial least squares-discriminant analysis (PLS-DA) for classification of high-dimensional (HD) data: a review of contemporary practice strategies and knowledge gaps, Analyst 143 (2018) 3526–3539, https://doi.org/10.1039/c8an00599k.
[30] E. Szymańska, E. Saccenti, A.K. Smilde, J.A. Westerhuis, Double-check: validation of diagnostic statistics for PLS-DA models in metabolomics studies, Metabolomics 8 (2012) 3–16, https://doi.org/10.1007/s11306-011-0330-3.
[31] USEPA, Nitrification, U.S. Environmental Protection Agency, USA, 2002.
[32] X. Zhang, D. Li, Y. Liang, H. Zeng, Y. He, Y. Zhang, J. Zhang, Performance and microbial community of completely autotrophic nitrogen removal over nitrite (CANON) process in two membrane bioreactors (MBR) fed with different substrate levels, Bioresour. Technol. 152 (2014) 185–191, https://doi.org/10.1016/j.biortech.2013.10.110.
[33] L.F. Pedersen, R. Oosterveld, P.B. Pedersen, Nitrification performance and robustness of fixed and moving bed biofilters having identical carrier elements, Aquac. Eng. 65 (2015) 37–45, https://doi.org/10.1016/j.aquaeng.2014.10.005.
[34] W. Jia, J. Zhang, Y. Lu, G. Li, W. Yang, Q. Wang, Response of nitrite accumulation and microbial characteristics to low-intensity static magnetic field during partial nitrification, Bioresour. Technol. 259 (2018) 214–220, https://doi.org/10.1016/j.biortech.2018.03.060.

[35] L. Tengrui, A.F. Al-Harbawi, L.M. Bo, Z. Jun, X.Y. Long, Characteristics of nitrogen removal from old landfill leachate by sequencing batch biofilm reactor, Am. J. Appl. Sci. 4 (2007) 211–214, https://doi.org/10.3844/ajassp.2007.211.214.
[36] O. Stavrakidis-Zachou, A. Ernst, C. Steinbach, K. Wagner, U. Waller, Development of denitrification in semi-automated moving bed biofilm reactors operated in a marine recirculating aquaculture system, Aquac. Int. 27 (2019) 1485–1501, https://doi.org/10.1007/s10499-019-00402-5.
[37] Y. Ruan, B. Ma, C. Cai, L. Cai, J. Gu, H.F. Lu, X.Y. Xu, M. Zhang, Kinetic affinity index informs the divisions of nitrate flux in aerobic denitrification, Bioresour. Technol. 309 (2020), 123345, https://doi.org/10.1016/j.biortech.2020.123345.
[38] R.C. Zhang, C. Chen, B. Shao, W. Wang, X.J. Xu, X. Zhou, Y.N. Xiang, L. Zhao, D. J. Lee, N.Q. Ren, Heterotrophic sulfide-oxidizing nitrate-reducing bacteria enables the high performance of integrated autotrophic-heterotrophic denitrification (IAHD) process under high sulfide loading, Water Res. 178 (2020), 115848, https://doi.org/10.1016/j.watres.2020.115848.
[39] M. Jiang, X. Zheng, Y. Chen, Enhancement of denitrification performance with reduction of nitrite accumulation and N2O emission by Shewanella oneidensis MR-1 in microbial denitrifying process, Water Res. 169 (2020), 115242, https://doi.org/10.1016/j.watres.2019.115242.
[40] Y. Gao, X. Wang, J. Li, C.T. Lee, P.Y. Ong, Z. Zhang, C. Li, Effect of aquaculture salinity on nitrification and microbial community in moving bed bioreactors with immobilized microbial granules, Bioresour. Technol. 297 (2020), 122427, https://doi.org/10.1016/j.biortech.2019.122427.
[41] H. Zhang, H. Wang, M. Jie, K. Zhang, Y. Qian, J. Ma, Performance and microbial communities of different biofilm membrane bioreactors with pre-anoxic tanks treating mariculture wastewater, Bioresour. Technol. 295 (2020), 122302, https://doi.org/10.1016/j.biortech.2019.122302.
[42] Y. Guan, H. Yang, S. Han, L. Feng, T. Wang, J. Ge, Comparison of the gut microbiota composition between wild and captive sika deer (Cervus nippon hortulorum) from feces by high-throughput sequencing, AMB Express 7 (2017) 1–13, https://doi.org/10.1186/s13568-018-0535-1.
[43] J.A. Fuerst, Phylum verrucomicrobia. Reference Module in Life Sciences, Elsevier,, 2019, https://doi.org/10.1016/B978-0-12-809633-8.20772-3.
[44] C. Solar, A. Escalona, D. Garrido, The gut microbiome after bariatric surgery. Microbiome and Metabolome in Diagnosis, Therapy, and other Strategic Applications, Elsevier,, 2019, pp. 235–242, https://doi.org/10.1016/B978-0-12-815249-2.00024-5.
[45] W. Luo, H.V. Phan, F.I. Hai, W.E. Price, W. Guo, H.H. Ngo, K. Yamamoto, L. D. Nghiem, Effects of salinity build-up on the performance and bacterial community structure of a membrane bioreactor, Bioresour. Technol. 200 (2016) 305–310, https://doi.org/10.1016/j.biortech.2015.10.043.
[46] H. Chang, P. Jin, X. Wang, X. Wang, The Study on Improvement of Nitrogen Removal by optimization of Aeration Mode, in: IWA 2017 Conf. Sustainable Wastewater Treatment and Resource Recovery: Research, Planning, Design and Operations, Chongqing, China, 2017: pp. 1–10.
[47] J. Ma, Z. Wang, Y. Yang, X. Mei, Z. Wu, Correlating microbial community structure and composition with aeration intensity in submerged membrane bioreactors by 454 high-throughput pyrosequencing, Water Res 47 (2013) 859–869, https://doi.org/10.1016/j.watres.2012.11.013.
[48] T.A. Smirnov, L.V. Didenko, I.G. Tiganova, S.G. Andreevskaya, N.V. Alekseeva, T. V. Stepanova, Y.M. Romanov, Study of the structures of biofilms formed by Salmonella typhimurium bacteria on abiotic surfaces by the methods of light and transmission electron microscopy, Appl. Biochem Microbiol 46 (2010) 706–711, https://doi.org/10.1134/s0003683810070057.
[49] A. Rodriguez-Sanchez, J.C. Leyva-Diaz, J.M. Poyatos, J. Gonzalez-Lopez, Influent salinity conditions affect the bacterial communities of biofouling in hybrid MBBR-MBR systems, J. Water Process Eng. 30 (2019), 100650, https://doi.org/10.1016/j.jwpe.2018.07.001.